Available online at www.sciencedirect.com

ScienceDirect

ELSEVIER

Physica E 40 (2008) 2278–2282

PHYSICA E

www.elsevier.com/locate/physe

# Hysteresis suppression in self-assembled single-wall nanotube field effect transistors

P. Hu*, C. Zhang, A. Fasoli, V. Scardaci, S. Pisana, T. Hasan, J. Robertson, W.I. Milne, A.C. Ferrari

*Department of Engineering, University of Cambridge, Cambridge CB3 0FA, UK*

Available online 04 December 2007

**Abstract**

We present a technique for hysteresis suppression in single-wall nanotube field effect transistors (SWNT-FETs) using chemical functionalization. We selectively modify the electrode surfaces and the device channel area with self-assembled monolayers (SAMs) of octanethiol and aminopropyltriethoxysilane (APTES), respectively. These can efficiently prevent surface adsorption of water molecules. We show that hysteresis is suppressed, with a 15 times decrease in hysteresis gap compared to the conventional SWNT-FETs on bare $SiO_2$/Si.

© 2007 Elsevier B.V. All rights reserved.

*PACS:* 73.63.Fg; 73.63.−b; 81.65.−b

*Keywords:* Nanotubes; Transistor; Hysteresis

## 1. Introduction

Single-wall carbon nanotube field-effect transistors (SWNT-FETs) are outstanding candidates for future nanoelectronics. To date, remarkable progress has been made in improving the ON/OFF ratio, carrier mobility and sub-threshold slope (*S*) by different approaches. These include (1) reduction of the gate oxide thickness [1]; (2) adoption of high-K gate dielectrics [2–4]; (3) use of electrolyte as gate dielectric [5,6]; (4) reduction of contact resistance using appropriate contact metals [7] and post-process treatments [8].

Hysteresis is an important performance factor for SWNT-FETs. During transfer characteristics (TCs) measurements, many SWNT-FETs exhibit hysteresis between the forward and reverse gate voltage sweeps, resulting in an apparent shift in the threshold voltage, sub-threshold slope and the current [9–12]. This is usually explained by charge injection from SWNTs into the oxide layer at large gate bias where the charges are trapped until the polarity is reversed [11–14]. Adsorbed molecules (e.g. water molecules) may also increase this effect by providing additional trap sites [10]. It has been reported that SWNT-FETs fabricated on $SiO_2$/Si substrates exhibit hysteresis in current versus gate–voltage characteristics (Si as back-gate) [12–14]. This was attributed either to charge traps in bulk $SiO_2$ [12], or to oxygen-related defect traps sites near SWNTs [13], or to traps at the $SiO_2$/Si interface [14]. Recently, the dependence of the hysteresis on the chemical environment was also investigated [10]. Ref. [10] attributes hysteresis to charge trapping from water molecules around the SWNTs, including $SiO_2$ surface-bound water molecules in close proximity to the SWNTs [10].

Hysteresis can be used for the development of memory devices [11–15]. However, SWNT-FET-based electronic applications (e.g. sensors [16–18], logic circuit [2,19,20]) require stable transport properties. Therefore, it is necessary to suppress hysteresis for such devices. Ref. [10] reported a technique to protect nanotube channels from ambient humidity by encasing the FET in a polymer. But such approach impedes further circuit integration of SWNT-FETs because the encased device is impossible to connect. Also, for applications such as sensing, this

*Corresponding author.
*E-mail address:* ph331@cam.ac.uk (P. Hu).

1386-9477/$ - see front matter © 2007 Elsevier B.V. All rights reserved.
doi:10.1016/j.physe.2007.11.034

technique is unsuitable since the encased FET cannot be functionalized with or exposed to chemicals and biomolecules. In this work, we demonstrate a new technique for hysteresis suppression by chemically functionalizing the surfaces where the SWNTs are deposited. This decreases the surface trap sites and prevents the adsorption of water molecules. In contrast to Ref. [10], our proposed method allows further integration of SWNT-FETs and their use in sensing.

## 2. Experimental

We consider two sets of SWNT-FETs: one with SWNTs directly deposited on the bare $SiO_2$/Si wafer (FET on $SiO_2$) and the other with SWNTs deposited on the $SiO_2$/Si coated with organic self-assembled monolayers (FET on SAM).

For FET on $SiO_2$, we grow SWNTs on $SiO_2$/Si using horse-spleen ferritin (Sigma-Aldrich) as the source of Fe catalyst [21]. Growth takes place in a 2-in diameter quartz tube furnace by heating up in an argon flow of 1000 sccm–900 °C. The growth is initiated by introducing methane at 500 sccm and hydrogen at 100 sccm. After 15 min, both the hydrogen and methane flows are stopped, and the furnace is purged and cooled down in argon flow. Cr/Au electrodes contacted with the as-grown SWNT on the wafer are then made using a conventional UV-lithography and lift-off. These Au electrodes have a thickness of 100 nm and a gap of 5–10 μm.

In the case of FETs on SAM, Cr/Au electrode patterns are made at first on n-type Si wafers with a 200 nm thermally oxidized layer, using the photolithography process mentioned above. The area between the electrodes (where SWNTs are to be deposited) is functionalized with a polar group (–$NH_3$) while the electrode surfaces with a non-polar group (–$CH_3$). The –$NH_3$ polar group is created by the following process: the $SiO_2$ surface between the electrodes is hydroxylated in a solution of ammonium hydroxide/hydrogen peroxide/water mixture; the hydroxyl group is then terminated with an amino group by immersing the wafer into 2% aminopropyltriethoxysilane (APTES) in an acetone/water mixture (95% /5%) for 1 h [22]. Subsequently, the surface of the Au electrodes is covered with a SAM of octanethiol by immersing the wafer in 2% methanol solution of octanethiol for 12 h. X-ray photoelectron spectrum (XPS) measurements are carried out on a JPS90-MX (JEOL) system, which is equipped with an angle-resolved hemispherical electron energy analyzer and a base system pressure of $1\text{–}10^{-9}$ Torr. All measurements are performed using the Al KR line with a photon energy of 1486.6 eV.

To selectively deposit SWNTs in the desired area, the above surface-modified wafer is immersed in a solution of SWNTs in 1,2-dichlorobenzene (~0.02 mg/ml) for 1 min. The device structure is checked by high-resolution scanning electron microscopy (SEM, FEI Philips XL30 sFEG). The electrical properties of SWNT FETs are measured using a HP 4156A semiconductor parameter analyser at ambient conditions.

To compare the electronic properties of the same device with/without SAM, the device is treated in air at 400 °C for 30 min and subsequently cooled in $N_2$.

## 3. Results and discussion

Fig. 1 plots the schematic structure of the FET on SAM with back gate used in this study. The SWNTs lie on the APTES modified Si/$SiO_2$ surface, contacting the two electrodes covered with octanethiol monolayer (source and drain). Previous studies showed that SWNTs tend to deposit in areas covered with polar chemicals when the wafer is dipped in a SWNT solution [23,24]. Since the area between our electrodes is functionalized with a polar APTES SAM, we find that the SWNTs are selectively deposited only on this area, as shown in Figs. 1 and 2. On the other hand, the Au electrodes are functionalized with non-polar octanethiol. Therefore, no SWNTs are deposited on the electrodes, as shown in Figs. 1 and 2.

Fig. 2 shows the morphology of the self-assembled SWNT-FET used in this work. SWNTs are deposited in the area between electrodes and contact the electrodes, while the surface of the gold electrode is clean, confirming selective deposition.

XPS are used to determine the selective functionalization. Nitrogen is present in the amino groups in APTES, whereas octanethiol does not have any nitrogen. We therefore assume the detection of nitrogen between electrodes to indicate APTES functionalization. XPS data (see Fig. 3) taken in an area between the electrodes indeed show the N 1s peak [22,25]. No nitrogen peak is detected on the surface of the gold electrodes.

To measure the TCs, the gate voltage ($V_G$) is swept forward and backward between $+V_G$ and $-V_G$ (in this study: $\pm 10$ V). The sub-threshold voltage ($V_{th}$) shifts to the right ($V^f_{th}$) for forward sweeps and to the left ($V^r_{th}$) for reverse sweeps. The hysteresis gap ($\Delta V_H = V^r_{th} - V^f_{th}$) is used

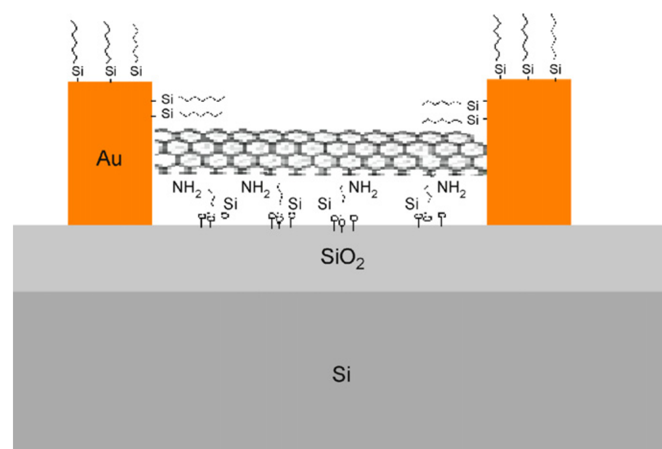


Fig. 1. Schematic structure of the self-assembled SWNT-FET from selective surface functionalization.

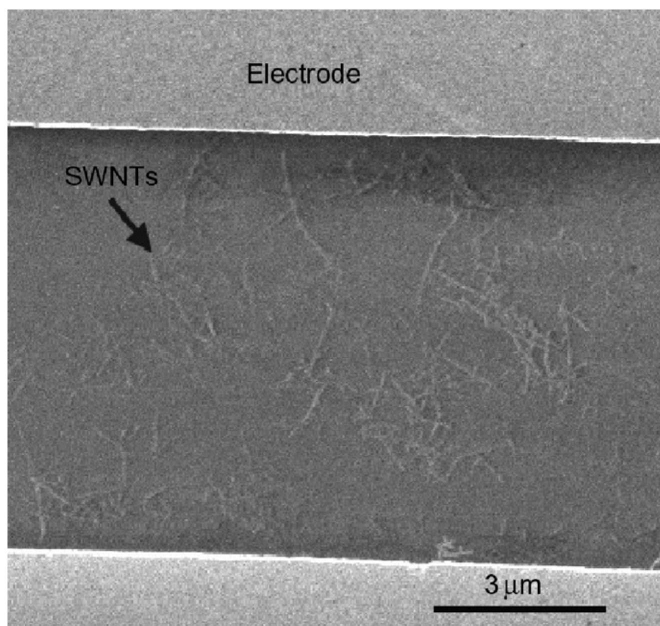


Fig. 2. SEM image of a FET device, showing SWNTs selectively deposited between electrodes.

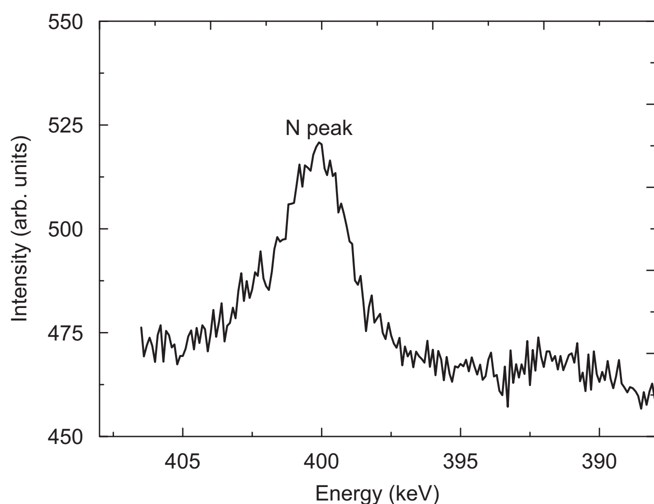


Fig. 3. X-ray photoelectron spectra (XPS) of N peak with binding energy of 400 eV.

to quantify the amount of hysteresis [11,12]. For this, the threshold voltage is defined as the gate voltage at $I_{DS} = 4$ nA.

To show efficiency in hysteresis suppression by our technique, the two typical SWNT-FETs (on bare $SiO_2$/Si substrate or SAM) are common in nanotubes (both from the same CVD procedure), electrode gap (10 μm), $SiO_2$/Si substrate (oxidized layer of 200 nm) and device operation (gate sweeping range of −10 to +10 v; gate sweeping speed: (1 V/s). Fig. 4a shows the TC in a typical FET on $SiO_2$ at room temperature. Here, $V_G$ is swept between −10 and +10 V in ≈20 s. A hysteresis loop is observed in the TC. The $\Delta V_H$ of this device is ≈8.4 V. Fig. 4b shows a typical TC of the FET on SAM. $V_G$ is also swept from −10 via +10 V in about 20 s. The hysteresis loop in the TC of FET on SAM nearly disappears. And the hysteresis gap ($\Delta V_H$) is only ≈0.5 V. Therefore, hysteresis is almost eliminated in the FET on SAM device.

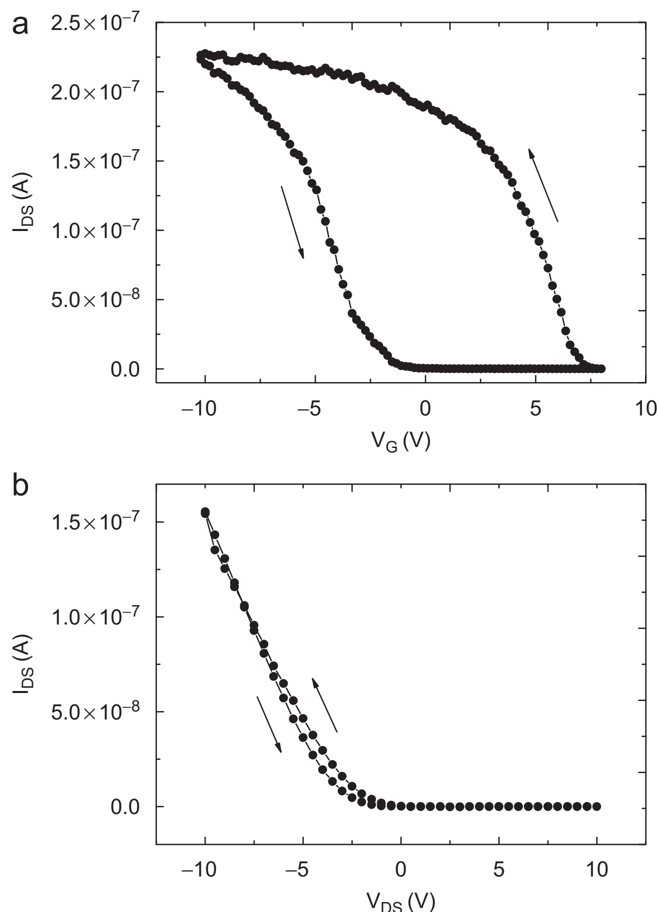


Fig. 4. (a) A typical transfer characteristic of SWNT-FETs lying directly on $SiO_2$/Si substrate with a large hysteresis loop; (b) a typical transfer characteristics of SWNT-FET lying on the SAM with a small hysteresis loop.

Water can provide charge trap sites [10]. The two possible origins of hysteresis from adsorbed water molecules in the SWNT-FET are: (1) water molecules weakly adsorbed on the SWNT surface [10] and (2) $SiO_2$ surface-bound water forms in close proximity to the SWNTs. The $SiO_2$ surface consists of Si–OH groups where water is adsorbed through a hydrogen bond to the silanol group [26,27]. Therefore, a layer of surface-bound water could exist in FET on $SiO_2$ if the device is stored in ambient air. In our FET on SAM, the hydrophobic APTES and octanethiol SAMs cover the surface of the device and thus prevent water adsorption. To further prove this, we tried to compare the transport properties of the same device with/without SAM. The device is treated in air at suitable temperature for a short time (350–400 °C). Only SAM is burned out and most of SWNTs are still there at this temperature, which is confirmed by XPS and SEM analysis. We measure the same device in different times: (1) before burning out the SAM; (2) shortly after it is

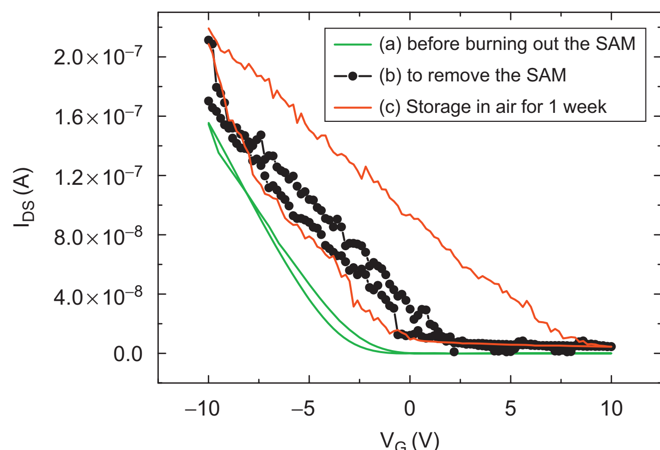


Fig. 5. Transfer characteristics of SWNT-FETs (a) with the SAM; (b) shortly after burning the SAM; (c) after having stored the device in air for 1 week.

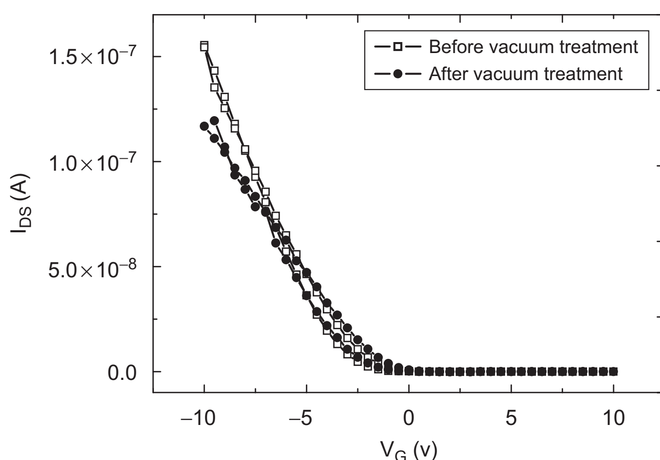


Fig. 6. Transfer characteristics of SWNT-FET lying on the SAM before vacuum treatment and after 36-h-vacuum treatment.

heated and cooled in $N_2$; (3) after storage in air for one week. The measure results are shown in Fig. 5. The FET on SAM shows a stable and minimum hysteresis for up to 5 months (Fig. 5a). When the device is heated and subsequently cooled in $N_2$, the device surface is still free of water and thus the FET shows a small hysteresis (Fig. 5b). After heat treatment, the device shows a little higher current (Fig. 5a, b), which is due to the improvement of the contact between nanotubes and electrodes after removal of octanethiol SAM. When the device is stored in the air for one week, water in air is absorbed to the $SiO_2$ surface via a hydrogen bond to the silanol group [26,27], so the FET shows a large hysteresis loop (shown in Fig. 5c). These results indicate the hysteresis in nanotube FET is mainly caused by water and hydrophobic SAMs can suppress the hysteresis efficiently.

To further study the origin of the remaining hysteresis in the FET on SAM devices, we try to remove any remaining surface water by keeping the device in vacuum for a prolonged period. We keep the FET on SAM device under vacuum for 36 h at 80 °C. Fig. 6 shows the TC of this device before and after the vacuum treatment. A small hysteresis is still observed even after the vacuum treatment. This implies that the origin of the remaining hysteresis is not due to the adsorbed water molecules since these should have been removed in the vacuum process. We attribute this to charge traps inside the underlying $SiO_2$/Si substrate as suggested in Refs. [12,13]. Gate voltages can produce a highly localized electric field around the nanotube surface. Since SWNTs have a small radius of curvature, charges are therefore easily and reversibly injected and removed from the $SiO_2$ dielectric when a bias voltage between the SWNTs and the substrate is applied [12,13].

## 4. Conclusions

We developed a technique to suppress hysteresis in SWNT-FET via a selective surface functionalization with SAMs. These hydrophobic SAMs can efficiently prevent surface adsorption of water molecules in SWNT-FETs. Compared to SWNT-FETs on bare $SiO_2$/Si surface, the hysteresis in SWNT-FETs on SAM is suppressed efficiently and the hysteresis gap in our experiments is reduced by a factor of about 15. These FETs on SAM deliver stable electric properties, and they are suited to be used for nanoscale biosensors [28].

## Acknowledgments

This work was supported by the Ministry of Information and Communication, Republic of Korea, under Project no. A1100-0602-0101. ACF acknowledges funding from the Royal Society and the Leverhulme Trust.

## References

[1] S.J. Wind, J. Appenzeller, R. Martel, V. Derycke, P. Avouris, Appl. Phys. Lett. 80 (2002) 3817.
[2] A. Bachtold, P. Hadley, T. Nakanishi, C. Dekker, Science 294 (2001) 1317.
[3] J. Appenzeller, J. Knoch, V. Derycke, R. Martel, S. Wind, P. Avouris, Phys. Rev. Lett. 89 (2002) 126 8011.
[4] A. Javey, H. Kim, M. Brink, Q. Wang, A. Ural, J. Guo, P. McIntyre, M. Lundstrom, H. Dai, Nat. Mater. 1 (2002) 241.
[5] S. Rosenblatt, Y. Yaish, J. Park, J. Gore, V. Sazonova, P.L. McEuen, Nano Lett. 2 (2002) 869.
[6] G.P. Siddons, D. Merchin, J.H. Back, J.K. Jeong, M. Shim, Nano Lett. 4 (2004) 927.
[7] J. Guo, D.B. Farmer, Q. Wang, E. Yenilmez, R.G. Gordon, M. Lundstrom, H. Dai, Nano Lett. 4 (2004) 1319.
[8] R. Martel, V. Derycke, C. Lavoie, J. Appenzeller, K.K. Chan, J. Tersoff, P. Avouris, Phys. Rev. Lett. 87 (2001) 256 805-1.
[9] A.R. Peillard, S.V. Rotkin, IEEE Trans. Nanotech. 4 (2005) 284.
[10] W. Kim, A. Javey, O. Vermesh, Q. Wang, Y. Li, H. Dai, Nano Lett. 3 (2003) 393.
[11] H. Lin, S. Tiwari, Appl. Phys. Lett. 89 (2006) 073507.
[12] M.S. Fuhrer, B.M. Kim, T. Dürkop, T. Brintlinger, Nano Lett. 2 (2002) 755.
[13] M. Radosavljevi, M. Freitag, K.V. Thadani, A.T. Johnson, Nano Lett. 2 (2002) 761.
[14] J.B. Cui, R. Sordan, M. Burghard, K. Kern, Appl. Phys. Lett. 81 (2002) 3260.

[15] S. Wanga, P. Sellin, Appl. Phys. Lett. 87 (2005) 133117.
[16] A.E. Star, T.J. Niemann, J.C.P. Gabriel, C.S.C. Joine, Proc. Natl. Acad. Sci. USA 103 (2006) 921.
[17] R.B. Chen, S. Bangsaruntip, K.A. Drouvalakis, N.W.S. Kam, M. Shim, Y. Li, W. Kim, P.J. Utz, H.J. Dai, Proc. Natl. Acad. Sci. USA 100 (2003) 4984.
[18] S. Sotiropoulou, N.A. Chaniotakis, Anal. Bioanal. Chem. 375 (2003) 103.
[19] P. Hu, K. Xiao, Y. Liu, G. Yu, X.B. Wang, L. Fu, G. Cui, D. Zhu, Appl. Phys. Lett. 84 (2004) 4932.
[20] Z. Chen, J. Appenzeller, Y.M. Lin, J. Sippel-Oakley, A.G. Rinzler, J. Tang, S.J. Wind, P.M. Solomon, P. Avouris, Science 377 (2006) 1735.
[21] Y. Li, W. Kim, Y. Zhang, M. Rolandi, D. Wang, H. Dai, J. Phys. Chem. B 105 (2001) 11424.
[22] G.J. Zhang, T. Tanii, T. Zako, T. Funatsu, I. Ohdomari, Sensors Actuators B 97 (2004) 243.
[23] J. Liu, M.J. Casavant, M. Cox, D.A. Walters, P. Boul, W. Lu, A.J. Rimberg, K.A. Smith, D.T. Colbert, R.E. Smalley, Chem. Phys. Lett. 303 (1999) 125.
[24] S.G. Rao, L. Huang, W. Setyawan, S. Hong, Nature 425 (2003) 36.
[25] J.F. Moulder, W.F. Stickle, P.E. Sobol, K.D. Bomben, Handbook of X-ray Photoelectron Spectroscopy, Perkin-Elmer Corporation, Eden Prairie, 1992.
[26] M.L. Hair, Infrared Spectroscopy in Surface Chemistry, Marcel Dekker, New York, 1967.
[27] L.T. Zhuravlev, Colloids Surf. A 173 (2000), 1–38.0.
[28] P. Hu, A. Fasoli, J. Park, Y. Choi, P. Estrela, P. Migliorato, W. I. Milne, A.C. Ferrari, submitted (2007).